Solar Energy 135 (2016) 618–624

Contents lists available at ScienceDirect

Solar Energy

journal homepage: www.elsevier.com/locate/solener

GaP/InGaAs/InGaSb triple junction current matched photovoltaic cell with optimized thickness and quantum efficiency

B. Tiwari, M.J. Hossain, I. Bhattacharya *

Department of Electrical and Computer Engineering, Tennessee Technological University, Cookeville, TN 38501, USA

ARTICLE INFO

Article history:
Received 23 February 2016
Received in revised form 11 June 2016
Accepted 13 June 2016

Keywords:
Multijunction solar cell
Quantum efficiency
High efficiency solar cell
Current matching

ABSTRACT

III–V multijunction solar cell technology demands high efficiency for its cost effective production. The proposed new combination of GaP/InGaAs/InGaSb triple junction solar cell is designed to convert more incident photons to electricity, executing higher internal quantum efficiency and promoting higher efficiency solar cells. The use of InGaSb (0.54 eV) as a bottom subcell layer empowers the collection of photons deeper in the infrared spectrum. The efficiency of the proposed multijunction solar cell is 23.53% under 1 sun concentration for AM 1.5 Global spectrum. This paper presents the optimization of quantum efficiency and current matching for each subcell layer with the change in thicknesses and doping concentrations. The work also maximizes open circuit voltage obtained from each of the subcell layers.

1. Introduction

The large gap between the potent of solar energy and utilization exists due to the higher cost and lower conversion capacity. Higher efficiency is one of the important attributes of a solar cell in making it more cost-effective. A crucial power loss mechanism in single bandgap cells is its inability to absorb photon with energy less than the bandgap and loss of energy of photons which has energy higher than the bandgap of the cell (Yamaguchi et al., 2005; Razykov et al., 2011). This process is responsible for significant amount of power loss in solar energy to electricity conversion (Ekins-Daukes, 2013; Xiong et al., 2010). Single junction solar cell efficiencies can be improved by effectively splitting the solar radiation spectrum, which can be done by two methods i.e. using beam-splitting filters and arranging the subcells in a mechanically stacked configuration called multijunction (MJ) or tandem systems (Imenes and Mills, 2004). Using the beam splitting filter, the light spectrum is distributed to locations, where the appropriate cells would be placed to collect the photons of certain energies (Imenes and Mills, 2004). The second and most preferred approach is stacking the subcells arranged so that the sunlight illuminates the highest bandgap subcell first and then progressively lower bandgap subcells (Yamaguchi et al., 2005). The stacked arrangement will avoid the requirement of any optical spectrum separator for distributing the radiation. This stacking of the solar cells with growing bandgap energies will increase the efficiency of the overall device because of the more incident photons being used to generate more electron-hole pairs. The high energy photons are absorbed by the higher bandgap subcell layers first and photons with lower energies will be passed to the lower bandgap subcell layers in the stack for absorption. As shown in Fig. 1, the higher energy photons are absorbed by cell with bandgap Eg1, similarly the middle cell with bandgap Eg2 absorbs the photons having energies equal to Eg2 but less than Eg1. The lowest subcell with bandgap Eg3 absorbs remaining lower energy photons. Here Eg1 > Eg2 > Eg3. It describes the working principle of multijunction solar cells. This type of configuration can be considered as filter acting as low-photon energy pass filter. The lower the bandgap of the materials the greater fraction of the incident photons will be absorbed producing higher current but lower voltage and vice versa (Derkacs et al., 2012). Therefore, we need to find the optimal balance between the photon absorption and voltage obtained.

Series connected/stacked subcell layer voltages add up and produce higher voltage than a single-junction solar cell. However, the current flowing through each subcell should be matched because of its series connection and reduce the temperature losses. This arrangement results in higher efficiency than single junction solar cells. Multijunction Concentrator Photovoltaics (CPV) has appeared as the most promising technology in solar cells, having record efficiency of 46% (±2.2%) for GaInP/GaAs and GaInAsP/GaInAs (508 Suns) (Green et al., 2016). The bandgap of the material has significant impact on the efficiency of photon absorption and voltage obtained. For better efficiency of a solar cell there should be the higher photon absorption and higher voltage obtained. In this paper a novel triple junction solar cell is introduced comprising GaP/$In_{0.2}Ga_{0.8}$ As/$In_{0.2}Ga_{0.8}Sb$ which uses InGaSb as a bottom subcell layer. InGaSb is also used as the substrate for proposed design

* Corresponding author.
E-mail address: ibhattacharya@tntech.edu (I. Bhattacharya).

http://dx.doi.org/10.1016/j.solener.2016.06.032
0038-092X/

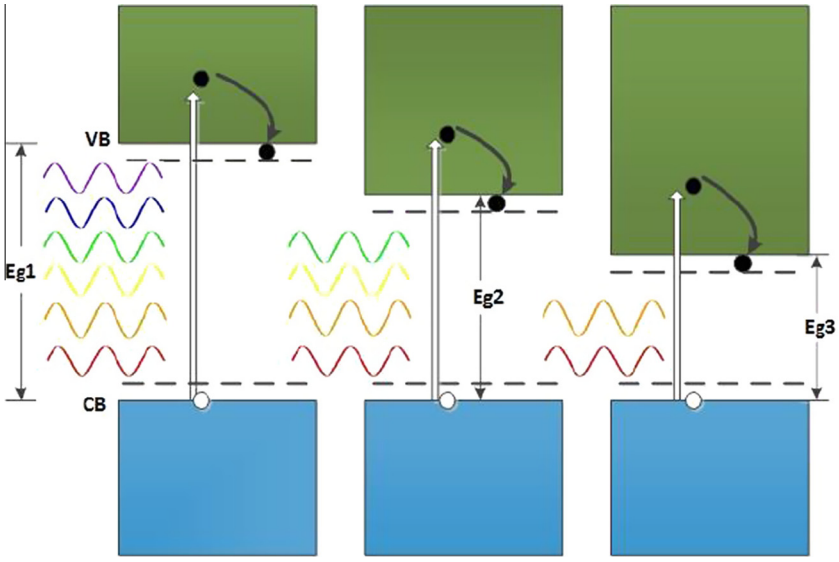

Fig. 1. Working principle of a multijunction solar cell where Eg1>Eg2>Eg3.

which is new in solar cell applications. We could see the application of InGaSb as a substrate in InGsSb photodetectors for 2 μm applications (Refaat et al., 2004). Compared to commonly used bottom subcell layer like Ge, InGaSb (0.54 eV) can absorb more photons in the deeper infrared region resulting in higher current. The thicknesses of the subcell layers were optimized to achieve quantum efficiencies for current matching, higher value of open circuit voltage and higher overall efficiency.

2. Proposed multijunction solar cell

Compound semiconductors are employed in fabricating multijunction solar cells. Materials selection with proper bandgaps is the most important criterion in designing high-efficiency solar cells. III–V semiconductor compounds have the potential to be stacked in different combinations because of its bandgap tunability through elemental composition. These compound semiconductor alloys have band gaps ranging from 0.3 to 2.3 eV, covering most of the solar spectrum (Leite et al., 2013). The proposed triple junction GaP/InGaAs/InGaSb is formed from the combination of III–V compounds with bandgaps of 2.26 eV/1.14 eV/0.54 eV respectively. Top cell with bandgap of 2.26 eV allows photons with energy less than 550 nm to be absorbed and create electron-hole pairs. Similarly, the middle cell with bandgap of 1.14 eV capture photons up to the wavelength of 1078 nm. Finally the bottom subcell will absorb photons up to the wavelength of 2250 nm contribute in photovoltaic conversion. Thus we can utilize wider spectrum of solar radiation (Bhattacharya and Foo, 2010; Tiwari et al., 2015).

2.1. Design perspective

An "infinite junction" solar cell can have a maximum theoretical efficiency of almost 87% (Yamaguchi and Luque, 1999). However, with increase in the number of junction the complexity and associated cost will escalate. Thus optimal balance between solar cell cost and efficiency is always preferred. Depending upon the choice of substrate, the epitaxial method, growth method and post-growth processing, the solar cell architecture and total cost is determined. The simplest and straight forward approach is to grow with lattice matched subcells and the substrate (Patel et al., 2012). However, selecting a proper band gap subcell layer even though they are lattice mismatched can still be grown using the metamorphic (MM) technologies. MM can be used in upright and inverted growth technique (King et al., 2005, 2012). Using the MM approach, bandgap of subcells can be chosen with more flexibility (Bett et al., 2013). The substrate and bottom subcell layer InGaSb having lattice constant of 6.1726 Å, over which the middle subcell layer InGaAs with lattice constant of 5.7342 Å is grown, the top layer GaP with lattice constant of 5.4505 Å is grown on top of the middle subcell. The proposed three subcell materials have lattice mismatch producing MM triple junction solar cell. Due to the difference in lattice constant, direct growth on top of the InGaSb bottom cell causes threading dislocations. This dislocation can be minimized by using the substantial buffer structures (King et al., 2007a,b). The middle subcell layer is made of $In_{(1-x)}Ga_xAs$ with $x = 0.8$ having bandgap of 1.14 eV. The bandgap is tuned given by the equation $0.36 + 0.63x + 0.43x^2$ (Adachi, 2009). The band gap equation of *InGaSb* bottom subcell layer with varying concentration is $In_{(1-x)}Ga_xSb = 0.170 + 0.135x + 0.415x^2$ where $x = 0.8$ (Adachi, 2009). The proposed multijunction solar cell with three subcells can be fabricated as shown in Fig. 2. Each subcell has a n-type emitter, p-type base, n-type window and a p-type back surface field. The base of each subcell is thicker than emitter, whereas the emitter is heavily doped in comparison to base. The heavily doped p-type back surface field will minimize the recombination of minority charge carriers and located on the rear side of each subcell (Narasimha et al., 1999). Two subcell are connected to each other using the heavily doped tunnel diodes. Tunnel junction should have higher transparency, so that light passes to the lower subcell layers. Tunnel diodes can be formed of materials with higher bandgap than the upper subcell, which offers less resistance to the flow of incident photons. Window layer used should have always higher bandgap than the subcells below and designed not to absorb any incident photons. To minimize the reflection of light from the surface of the solar cell, anti-reflective coating layer is used. It helps to increase the power conversion efficiency because of its efficient transmission of incident light to the absorbing semiconductor layers (Saylan et al., 2015). The electrical circuit equivalent of the proposed triple junction solar cell is shown in Fig. 3. The top p–n junction diode has the highest bandgap energy, thus collects light from the shorter wavelengths. Photons with energy lower than the bandgap energy pass to the lower junctions. The tunnel junctions are represented by the diode which are arranged

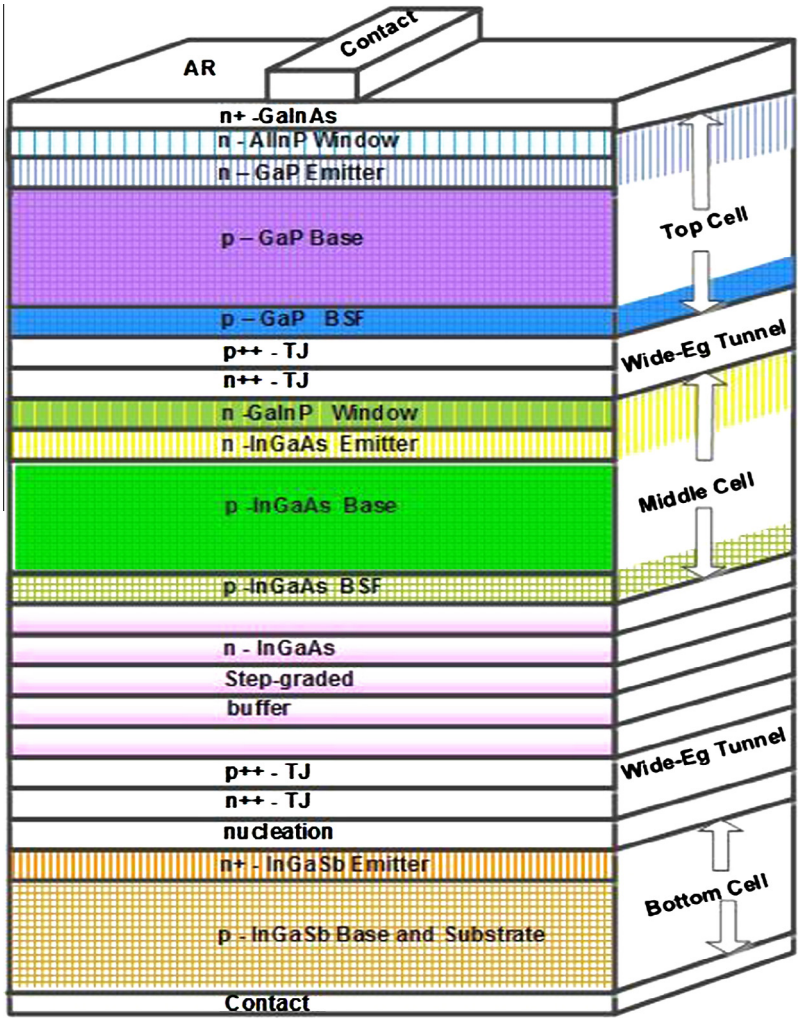

Fig. 2. Metamorphic design of the triple junction solar cell.

in the reverse polarity to the subcell diode. The dopant concentration for different n and p type of each subcell is considered to be in the order of $10^{21}/cm^3$ and $10^{20}/cm^3$.

The Internal Quantum Efficiency (IQE) is defined as the number of charge carriers generated by solar cell to the number of photons of a given energy absorbed by the solar cell. Our assumptions for simplification (Wanlass et al., 1991; Kurtz et al., 1990) include (a) transparent zero resistance tunnel junction interconnects, (b) no reflection losses, (c) no series resistance losses and (d) all subcell's current–voltage curves are described by the ideal ($n = 1$) diode equation. The Quantum Efficiency of an ideal cell of a base thickness x_b, emitter thickness x_e, and depletion width W is given by Eq. (1) (Luque and Hegedus, 2011). $\alpha(\lambda)$ is absorption coefficient, L_b, S_b and D_b are diffusion length, surface recombination velocity and diffusivity of base. L_e, S_e and D_e are diffusion length, surface recombination velocity and diffusivity of emitter.

$$QE = QE_{emitter} + QE_{depl} + QE_{base} \times \exp\left(-\alpha(x_e + W)\right) \tag{1}$$

$$QE_{emitter} = f_{\alpha}(L_e)\left(\frac{l_e + \alpha L_e - \exp(-\alpha x_e) \times \left[l_e \cosh\left(\frac{x_e}{L_e}\right) + \sinh\left(\frac{x_e}{L_e}\right)\right]}{l_e \sinh\left(\frac{x_e}{L_e}\right) + \cosh\left(\frac{x_e}{L_e}\right)} - \alpha L_e \exp(-\alpha x_e)\right) \tag{2}$$

$$QE_{depl} = \exp(-\alpha x_e)[1 - \exp(-\alpha W)] \tag{3}$$

$$QE_{base} = f_{\alpha}(L_b)\left(\alpha L_b - \frac{l_b \cosh\left(\frac{x_b}{L_b}\right) + \sinh\left(\frac{x_b}{L_b}\right) + (\alpha L_b - l_b)\exp(-\alpha x_b)}{l_b \sinh\left(\frac{x_b}{L_b}\right) + \cosh\left(\frac{x_b}{L_b}\right)}\right) \tag{4}$$

where $f_{\alpha}(L) = \alpha L/(\alpha L)^2 - 1$, $l_e = \frac{S_e L_e}{D_e}$, $l_b = \frac{S_b L_b}{D_b}$

For multijunction solar cell, the solar spectrum incident on each subcell depends on properties of other subcells lying above it. The top cell will have incident of full solar spectrum $\varnothing_s$. However, light hitting the mth subcell is filtered by junction above it and mth subcell sees an incident spectrum given by Eq. (5) (Luque and Hegedus, 2011).

$$\varnothing_m(\lambda) = \varnothing_s(\lambda) \exp\left[-\sum_{i=1}^{m-1} \alpha_i(\lambda) x_i\right] \tag{5}$$

The short-circuit current density (Jsc) of each subcell is determined by the Quantum efficiency of each layer and the spectrum of light incident (ϕ_{Inc}) on the solar cell given by Eq. (6)

$$J_{SC} = e \int_0^{\infty} (QE(\lambda)\varnothing_{Inc}(\lambda)d\lambda) \tag{6}$$

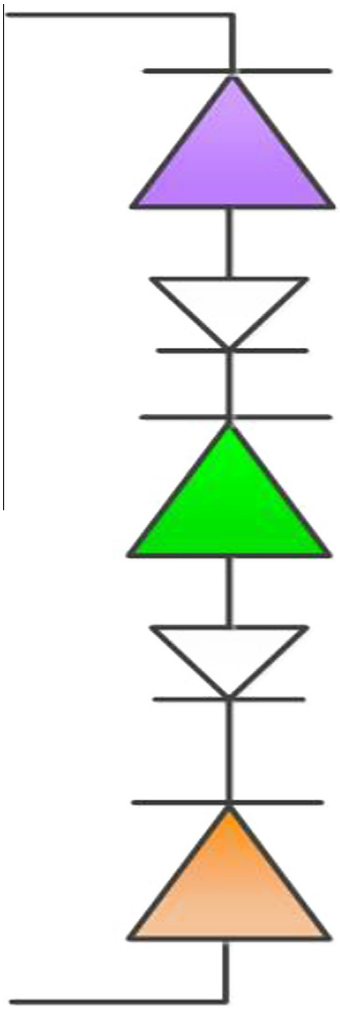

Fig. 3. Triple junction solar cell with its electrical circuit equivalent.

2.2. Optimization of quantum efficiency

Quantum Efficiency (QE) of a subcell layer is the ratio of the number of electron hole pair created to the number of photons absorbed (Park et al., 2009). We wanted to maximize QE to increase the efficiency of the proposed solar cell. Each subcell layer absorbs photons with certain energies of the incident spectrum. In the process of optimization, we optimized emitter thicknesses, base thicknesses, keeping the life time and surface recombination velocities constant to achieve higher QE and overall efficiency. We considered the QE curve of each subcell to be shielded for the range of the covered spectrum to minimize the overlapping of the curves. The chosen thicknesses for our proposed current matched MJ solar cell and the corresponding QE curve is shown in Figs. 4–6 respectively. The red color curve is finally plotted against the incident AM 1.5 global spectrum in Fig. 7. For GaP subcell, we selected the thickness parameters such that we obtain maximum QE possible and thus maximum current was extracted supported by Eq. (6). Top subcell current is critical for our case because its current value bounds the overall device current and thus limits efficiency. The maximum QE for GaP subcell was obtained for emitter thickness of 3.5 μm and base thickness of 6.85 μm. The middle subcell QE was optimized considering the thicknesses of the top subcell and the photons absorbed by the top subcell. We observed in most of the cases as we increase the base thicknesses, QE increases until a certain limit whereas,

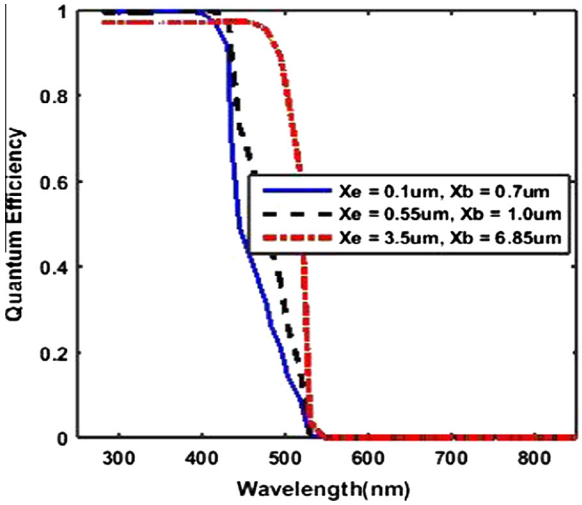

Fig. 4. Quantum Efficiency of GaP (2.26 eV) for different thicknesses.

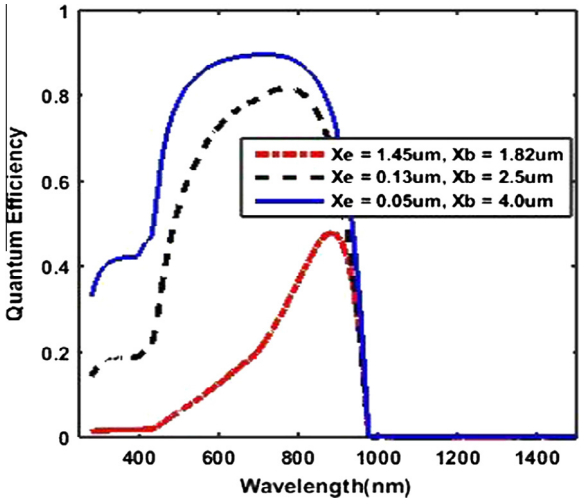

Fig. 5. Quantum Efficiency of InGaAs (1.14 eV) for different thicknesses.

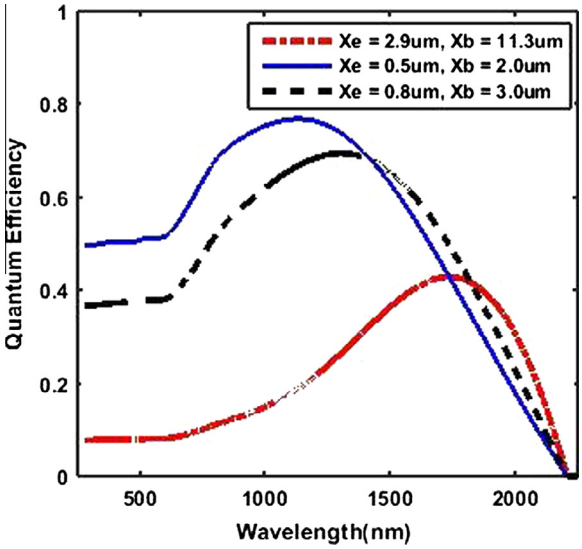

Fig. 6. Quantum Efficiency of InGaSb (0.54 eV) for different thicknesses.

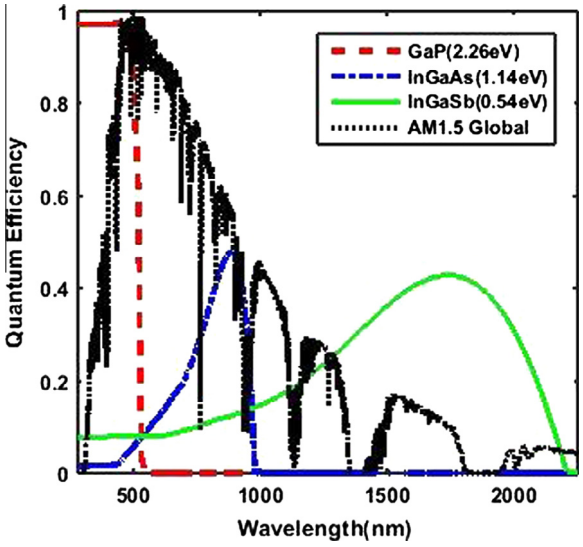

Fig. 7. Optimized QE for all three subcell layers plotted on top of normalized AM1.5 Global spectrum radiation for the case of current matched among subcells.

with increase in emitter thickness decreases the QE. The suitable thickness for middle subcell considering the current matching criteria for all subcell was emitter thickness of 1.45 μm and base thickness of 1.82 μm. Although it is evident that the better QE for middle subcell is obtained for emitter thickness = 0.05 μm and base thickness of 4.0 μm as shown in Fig. 5. For the bottom subcell we found the optimized thickness of emitter and base to be 2.9 μm and 11.3 μm respectively.

The different cases for thicknesses for each subcell layers and corresponding output parameters such as current density, voltage and efficiency is calculated as shown in Table 1 which is explained later on Section 2.3.

2.3. Multijunction J–V curves

For a given *m*-junction solar cell connected in series, its overall voltage is given by the summation of individual voltage across each subcell as in Eq. (7). However, for the same amount of current should follow through all the subcells. The total voltage of MJ solar cell with *m* junction is

$$V_{total} = \sum_{i=1}^{m} V_i \tag{7}$$

Since the solar cell is considered as a Photo-diode, its *J–V* characteristics is given by Eq. (8).

$$J = J_o[\exp(eV/nK_BT) - 1] - J_{SC} \tag{8}$$

where J_o is dark current density, e is the electron charge, K_B is the Boltzmann constant, V is the voltage, T is the temperature, J_{SC} is the short circuit current and n is the diode ideality factor. For our case we consider ideal diode with $n = 1$. To find the open circuit voltage (Voc), we utilized Eq. (9) and for the Fill factor calculation, we used the empirically determined formula of Eq. (10) (Green, 1981).

$$V_{OC} \approx (kT/e)\ln(J_{SC}/J_o) \tag{9}$$

$$FF = \frac{V_{OCnormalised} - \ln(V_{OCnormalised} + 0.72)}{V_{OCnormalised} + 1} \text{ Where }, V_{OCnormalised} = \frac{q}{nkT} V_{OC} \tag{10}$$

The overall power conversion efficiency of a solar cell is given by

$$\eta = \frac{J_{sc} \times V_{oc} \times FF}{P_{incident}} \times 100\% \tag{11}$$

where $P_{incident}$ is the input power to the solar cell. For AM 1.5 Global solar spectrum we considered incident power as 1000 W/m^2.

The current density vs voltage curve is shown in Fig. 8 for unmatched current through each subcell. Parameters such as emitter and base thickness for this plot is depicted in case '1' of the Table 1. Current density of top subcell was found to be 6.2 mA/cm^2, open circuit voltage (Voc) to be 2.0 V and efficiency of 20.10% for a cumulative thickness of 15.25 μm for emitter and base. It is evident from the plot that the top layer current value is decisive in determining the current generation from other subcells because of current matching constraints. Our design approach was to maximize the current density of GaP subcell layer at first. We increased the base thickness in case '2' to increase the Quantum Efficiency (QE) of base, which increased the current density to 6.7 mA/cm^2. This led to decrease in the voltage by 8 mV because of increase in dark current density J_0 as supported by Eq. (9). The increase in overall thickness of top cell results in decrease of current density of middle subcell layer to 14.3 mA/cm^2 from 14.5 mA/cm^2. This decrease in current is due to lesser number of photons incident on middle subcell as supported by Eq. (5). Similarly for case '3' current density of top cell rises to 7.2 mA/cm^2 and thus overall efficiency to 23.43% by increasing the emitter QE as backed by Eq. (6). For case '4' we are able to find the parameters for the maximum possible current density of the top GaP layer, which produces 7.4 mA/cm^2, however Voc decreases to 1.988 V. We fixed these parameters for GaP subcell layer and tried to match the current density of 7.4 mA/cm^2 for other two subcell layers; maintaining minimum drop in the Voc across each subcell. Due to the increase in thickness of upper subcells, photons incident on lower subcells decreases; hence the current density of middle cell decreases from 14.5 mA/cm^2 to 8 mA/cm^2 and bottom subcell from 18.5 mA/cm^2 to 7.4 mA/cm^2 respectively. From case '1'-'4'of Table 1, current density through each subcell aren't matched, however we calculated the efficiency of overall cell by considering the minimum short circuit current out of three subcells as our Jsc. This provides the prospective insight to the designers about the important layers to be considered and approximate the overall

Table 1
Optimization of quantum efficiency & conversion efficiency.

Case	GaP (2.26 eV)				InGaAs (1.14 eV)				InGaSb (0.54 eV)				Total thickness μm	Conversion efficiency (η)
	x_e μm	x_b μm	$\lvert J_{SC1}\rvert \frac{mA}{cm^2}$	V_{OC1} V	x_e μm	x_b μm	$\lvert J_{SC2}\rvert \frac{mA}{cm^2}$	V_{OC2} V	x_e μm	x_b μm	$\lvert J_{SC3}\rvert \frac{mA}{cm^2}$	V_{OC3} V		
1	0.15	3.0	6.2	2.000	0.5	3.0	14.5	0.961	0.6	8.0	18.5	0.4285	15.25	20.10%
2	0.15	5.0	6.7	1.992	0.5	3.0	14.3	0.961	0.6	8.0	18.5	0.4285	17.25	21.65%
3	2.5	5.0	7.2	1.993	0.5	3.0	14.3	0.961	0.6	8.0	18.5	0.4285	19.60	23.43%
4	3.5	6.85	7.4	1.988	1.40	3.0	8.0	0.939	2.8	3.0	7.4	0.3961	20.55	23.40%
5	3.5	6.85	7.4	1.988	1.55	3.0	7.4	0.936	2.8	3.0	7.4	0.3960	20.70	23.36%
6	3.5	6.85	7.4	1.988	1.55	3.0	7.4	0.936	2.8	3.5	7.4	0.3971	21.20	23.47%
7	3.5	6.85	7.4	1.989	1.45	1.82	7.4	0.936	2.9	11.3	7.4	0.3993	27.82	23.53%

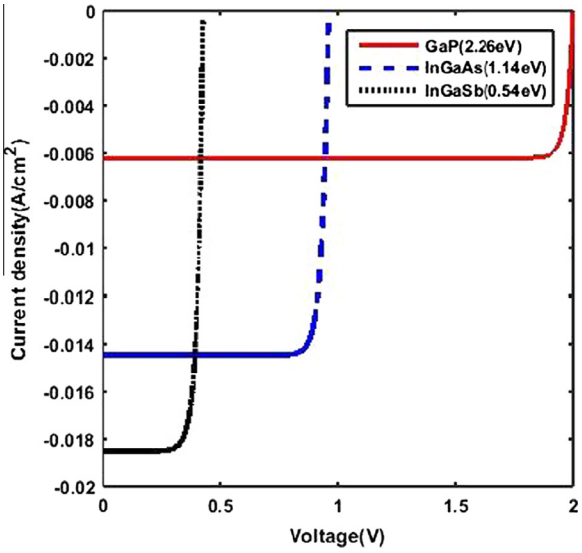

Fig. 8. *J–V* curve measured for GaP (2.26 eV)/InGaAs (1. 14 eV)/InGaSb (0.54 eV) multijunction configuration with unmatched current.

performance of multijunction solar cells. The current matched triple junction solar cell configuration extracted 7.4 mA/cm^2 from all subcells in the case of '5'-'7'. Although the open circuit voltage dropped by 12 mV, 25 mV and 32.5 mV for top, middle and bottom subcells respectively we were able to get higher overall efficiency. Case '5' the current matched multijunction solar cell have the efficiency of 23.36% with total emitter and base thickness of 20.70 μm. For same current density of 7.4 mA/cm^2, we were able to increase the open circuit voltage (Voc) by increasing the thickness of base of third subcell and consequently decrease in J_0 to reach efficiency of 23.47% with cumulative thickness of emitter and base of 21.20 μm. The maximum efficiency for our proposed GaP(2.26 eV)/InGaAs(1.14 eV)/InGaSb(0.54 eV) was calculated to be 23.53% with Jsc of 7.4 mA/cm^2 and Voc 3.3243 V for a total emitter and base thickness 27.82 μm. The current density vs voltage for this parameters are plotted Fig. 9.

We saw from the plot of *J–V* curve in Fig. 8 the middle and bottom subcells could generate current densities of 14.5 mA/cm^2 and 18.5 mA/cm^2 as calculated in case '2', considering the tandem

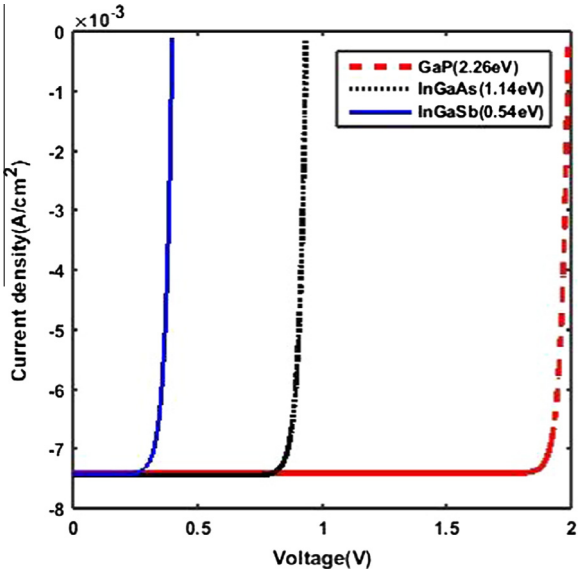

Fig. 9. *J–V* curve measured for GaP (2.26 eV)/InGaAs (1.14 eV)/InGaSb (0.54 eV) multijunction solar cell with current matched.

configuration. However, we are obligated to use those subcells below par their capacity because of the current density limit set by the top cell to 7.4 mA/cm^2. Thus we realized the importance of selecting the proper bandgap materials and the order of their placement in a multijunction solar cell to achieve maximum power conversion.

3. Conclusion

In this paper a triple junction solar cell comprising subcell layers GaP (2.26 eV)/InGaAs (1.14 eV)/InGaSb (0.54 eV) is proposed. Individual subcell's QE was optimized according to the thickness of emitter and base, after which it was optimized to obtain current matching through each subcell layers. The current density, voltage and the overall efficiency was calculated under 1-sun concentration for AM1.5 Global spectrum. Important semiconductor parameters such as thicknesses of emitter and base layers, doping concentrations, minority carrier lifetimes and surface recombination velocities were considered. The design offers cost reduction in multijunction solar cells using cost-effective materials. InGaSb has the lower material cost compared to the widely used bottom subcell layer Ge and can absorb more photons in the infrared range compared to Ge. We can interpret from the results that thickness of emitter and base plays a pivotal role in determining the overall performance of each subcell.

References

Adachi, S., 2009. Properties of Semiconductor Alloys: Group-IV, III-V and II-VI Semiconductors. John Wiley & Sons.

Bett, A.W., Philipps, S.P., Essig, S., Heckelmann, S., Kellenbenz, R., Klinger, V., Niemeyer, M., Lackner, D., Dimroth, F., 2013. Overview about technology perspectives for high efficiency solar cells for space and terrestrial applications. In: 28th European Photovoltaic Solar Energy Conference and Exhibition, p. 1.

Bhattacharya, I., Foo, S.Y., 2010. Effects of gallium-phosphide and indium-gallium-antimonide semiconductor materials on photon absorption of multijunction solar cells. IEEE SoutheastCon 2010 (SoutheastCon), Proceedings of the, pp. 316–319.

Derkacs, D., Jones-Albertus, R., Suarez, F., Fidaner, O., 2012. Lattice-matched multijunction solar cells employing a 1 eV GaInNAsSb bottom cell. J. Photonic. Energy 2 (1), 021805-1–021805-8.

Ekins-Daukes, N., 2013. Routes to high efficiency photovoltaic power conversion. In: Photovoltaic Specialists Conference (PVSC), 2013 IEEE 39thIEEE, p. 0013.

Green, M.A., 1981. Solar cell fill factors: general graph and empirical expressions. Solid-State Electron. 24 (8), 788–789.

Green, M.A., Emery, K., Hishikawa, Y., Warta, W., Dunlop, E.D., 2016. Solar cell efficiency tables (version 47). Prog. Photovoltaics Res. Appl. 24 (1), 3–11.

Imenes, A., Mills, D., 2004. Spectral beam splitting technology for increased conversion efficiency in solar concentrating systems: a review. Sol. Energy Mater. Sol. Cells 84 (1), 19–69.

King, R.R., Law, D.C., Edmondson, K.M., Fetzer, C.M., Kinsey, G.S., Yoon, H., Krut, D.D., Ermer, J.H., Sherif, R.A., Karam, N.H., 2007a. Metamorphic concentrator solar cells with over 40% conversion efficiency. Globe 1, 7.

King, R., Bhusari, D., Larrabee, D., Liu, X., Rehder, E., Edmondson, K., Cotal, H., Jones, R., Ermer, J., Fetzer, C., 2012. Solar cell generations over 40% efficiency. Prog. Photovoltaics Res. Appl. 20 (6), 801–815.

King, R.R., Law, D., Edmondson, K., Fetzer, C., Kinsey, G., Yoon, H., Sherif, R., Karam, N., 2007b. 40% efficient metamorphic GaInP/GaInAs/Ge multijunction solar cells. Appl. Phys. Lett. 90 (18), 183516-183516-3.

King, R., Sherif, R., Kinsey, G., Kurtz, S., Fetzer, C., Edmondson, K., Law, D., Cotal, H., Krut, D., Ermer, J., 2005. Bandgap engineering in high-efficiency multijunction concentrator cells. Cell 30, 40.

Kurtz, S.R., Faine, P., Olson, J., 1990. Modeling of two-junction, series-connected tandem solar cells using top-cell thickness as an adjustable parameter. J. Appl. Phys. 68 (4), 1890–1895.

Leite, M.S., Woo, R.L., Munday, J.N., Hong, W.D., Mesropian, S., Law, D.C., Atwater, H. A., 2013. Towards an optimized all lattice-matched InAlAs/InGaAsP/InGaAs multijunction solar cell with efficiency > 50%. Appl. Phys. Lett. 102 (3), 033901.

Luque, A., Hegedus, S., 2011. Handbook of Photovoltaic Science and Engineering. John Wiley & Sons.

Narasimha, S., Rohatgi, A., Weeber, A., 1999. An optimized rapid aluminum back surface field technique for silicon solar cells. Electron Devices, IEEE Trans. 46 (7), 1363–1370.

Park, S.H., Roy, A., Beaupre, S., Cho, S., Coates, N., Moon, J.S., Moses, D., Leclerc, M., Lee, K., Heeger, A.J., 2009. Bulk heterojunction solar cells with internal quantum efficiency approaching 100&percnt. Nat. Photonic. 3 (5), 297–302.

Patel, P., Aiken, D., Boca, A., Cho, B.Y., Chumney, D., Clevenger, M., Cornfeld, A., Fatemi, N., Lin, Y., McCarty, J., 2012. Experimental results from performance improvement and radiation hardening of inverted metamorphic multijunction solar cells. Photovoltaics, IEEE J. 2 (3), 377–381.

Razykov, T., Ferekides, C., Morel, D., Stefanakos, E., Ullal, H., Upadhyaya, H., 2011. Solar photovoltaic electricity: current status and future prospects. Sol. Energy 85 (8), 1580–1608.

Refaat, T., Abedin, M.N., Bhagwat, V., Bhat, I.B., Dutta, P.S., Singh, U.N., 2004. InGaSb photodetectors using an InGaSb substrate for 2 m applications. Appl. Phys. Lett 85 (11), 1874–1876.

Saylan, S., Milakovich, T., Hadi, S.A., Nayfeh, A., Fitzgerald, E.A., Dahlem, M.S., 2015. Multilayer antireflection coating design for GaAs 0.69 P 0.31/Si dual-junction solar cells. Sol. Energy 122, 76–86.

Tiwari, B., Penumaka, R., Bhattacharya, I., Mahajan, S.M., Foo, S., 2015. A novel GaP/InGaAs/InGaSb triple junction photovoltaic cell with optimized quantum efficiency. Photovoltaic Specialist Conference (PVSC), 2015 IEEE 42ndIEEE, p. 1.

Wanlass, M., Coutts, T., Ward, J., Emery, K., Gessert, T., Osterwald, C., 1991. Advanced high-efficiency concentrator tandem solar cells. In: Photovoltaic Specialists Conference, 1991, Conference Record of the Twenty Second IEEEIEEE, p. 38.

Xiong, K., Lu, S., Dong, J., Zhou, T., Jiang, D., Wang, R., Yang, H., 2010. Light-splitting photovoltaic system utilizing two dual-junction solar cells. Sol. Energy 84 (12), 1975–1978.

Yamaguchi, M., Takamoto, T., Araki, K., Ekins-Daukes, N., 2005. Multi-junction III–V solar cells: current status and future potential. Sol. Energy 79 (1), 78–85.

Yamaguchi, M., Luque, A., 1999. High efficiency and high concentration in photovoltaics. Electron Devices, IEEE Trans. 46 (10), 2139–2144.